

# Shear and Bulk Viscosities of Quark Matter from Quark-Meson Fluctuations in the Nambu–Jona-Lasinio model

Sabyasachi Ghosh<sup>1</sup>, Thiago C. Peixoto<sup>1</sup>, Victor Roy<sup>2</sup>, Fernando E. Serna<sup>1</sup>, and Gastão Krein<sup>1</sup>

<sup>1</sup>*Instituto de Física Teórica, Universidade Estadual Paulista,  
Rua Dr. Bento Teobaldo Ferraz, 271 - Bloco II, 01140-070 São Paulo, SP, Brazil and*

<sup>2</sup>*Institut für Theoretische Physik, Johann Wolfgang Goethe-Universität,  
Max-von-Laue-Str. 1, D-60438 Frankfurt am Main, Germany*

We have calculated the temperature dependence of shear  $\eta$  and bulk  $\zeta$  viscosities of quark matter due to quark-meson fluctuations. The quark thermal width originating from quantum fluctuations of quark- $\pi$  and quark- $\sigma$  loops at finite temperature is calculated with the formalism of real-time thermal field theory. Temperature-dependent constituent-quark and meson masses, and quark-meson couplings are obtained in the Nambu–Jona-Lasinio model. We found a non-trivial influence of the temperature-dependent masses and couplings on the Landau-cut structure of the quark self-energy. Our results for the ratios  $\eta/s$  and  $\zeta/s$ , where  $s$  is the entropy density (also determined in the Nambu–Jona-Lasinio model in the quasi-particle approximation), are in fair agreement with results of the literature obtained from different models and techniques. In particular, our result for  $\eta/s$  has a minimum very close to the conjectured AdS/CFT lower bound,  $\eta/s = 1/4\pi$ .

PACS numbers: 12.38.Mh, 25.75.-q, 25.75.Nq, 11.10.Wx, 51.20+d, 51.30+i

## I. INTRODUCTION

A high-temperature, weakly interacting medium is naturally expected to be produced in heavy ion collision (HIC) experiments at high energies because the constituents of the medium (quarks and gluons) should become almost free according to the asymptotic freedom property of quantum chromodynamics (QCD). However, the experimental finding of elliptic flow in HICs at the Relativistic Heavy Ion Collider (RHIC) leads to the interpretation that the medium produced in the collisions is actually a strongly interacting liquid, instead of a weakly interacting gas. This interpretation comes, in first place, from the ability of hydrodynamics to describe the RHIC data with a small value of the shear viscosity over entropy density ratio,  $\eta/s$  [1–8]. The shear viscosity coefficient  $\eta$  of a medium represents the ability of its constituents to transfer momentum over a distance comparable to their mean free path. When the inter-particle coupling is strong, momentum transfer takes place easily and, therefore, the shear viscosity of the matter is small. Several theoretical studies have estimated the ratio  $\eta/s$ , at weak and strong couplings and for different temperature regimes — a set of such studies is represented by Refs. [9–36, 38–42]. For earlier studies, see e.g. Refs. [43–46]. An interesting feature of the results in Refs. [15, 16, 21, 28] is that  $\eta/s$  reaches a minimum in the vicinity of a phase transition; the smallness of this minimum is significant in connection with a conjectured lower bound,  $\eta/s = 1/4\pi$ , known as the KSS bound, obtained in the context of AdS/CFT correspondence [47].

Similar to the shear viscosity, another transport coefficient is the bulk viscosity,  $\zeta$ . It is defined as the proportionality constant between the non-zero trace of the viscous stress tensor to the divergence of the fluid velocity, and usually it appears associated with processes accompanied by a change in fluid volume or density. The

bulk viscosity has received much less attention than the shear viscosity in hydrodynamical simulations because its numerical value is assumed to be very small, as it is directly proportional to the trace of the energy-momentum tensor which generally vanishes for conformally symmetric matter. However, lattice QCD simulations [48, 49] have shown that the trace of the energy momentum tensor of hot and dense QCD might be large near the QCD phase transition, which in turn indicates a non-zero, and possibly large value of  $\zeta$  as well as of  $\zeta/s$  near the transition temperature. In the framework of pure-gauge lattice QCD,  $\zeta/s$  near the transition temperature is estimated in Ref. [50]. Analytical calculations employing different techniques and models have been used for estimating  $\zeta$  of strongly interacting matter, a list of references are [26, 34, 51–61]; some of those [51–53] indicate a divergent behavior for  $\zeta$  near the transition temperature.

In this work we employ the two-flavor Nambu–Jona-Lasinio (NJL) model [62] to evaluate the temperature dependence of the shear and bulk viscosities in the vicinity of the crossover temperature. The NJL model is a very useful model for studying many aspects of the chiral structure of QCD in vacuum and at finite temperature and baryon density [63]. The model has also brought a great deal of insight into the problem of viscosities of strongly interacting matter [26, 34–36, 42, 45, 61]. A practical and transparent way to evaluate the contributions of quark-meson fluctuations to viscosities is to evaluate one-loop quark self-energy diagrams to obtain the quark relaxation time or, equivalently, the quark thermal width [35, 36]. Adopting this method, we have first analyzed the detailed Landau cut structures of the quark self-energy for quark- $\pi$  and quark- $\sigma$  loops, where the temperature dependence of the quark and meson masses and their couplings play an important role for its on-shell contributions. The present work explicitly demonstrates the nontrivial contributions of the temperature depen-

dence and momentum dependence of the quark thermal width to the viscosities, in the kinematic domains where the quark pole remains within the regions of the Landau cut. The new aspect explored in the present work relates to the contributions of quark- $\sigma$  and quark- $\pi$  fluctuations to  $\eta$  and  $\zeta$ , which become the main sources of dissipation beyond temperatures where pion decay into on-shell quark-antiquark pairs becomes possible. This temperature is commonly known as Mott temperature ( $T_M$ ) above which the threshold condition of pion dissociation i.e.  $m_\pi(T) > 2M_Q(T)$  is satisfied. In a very recent work [64], the NJL model was used to investigate the role played by quark-meson fluctuations on the shear viscosity. Our work is complementary to that one, as we use a different formalism to evaluate viscosities, consider also the bulk viscosity, use different quark- $\pi$  and quark- $\sigma$  couplings reflecting dynamical chiral symmetry breaking, and make a detailed study of the Landau cut structure of the quark self-energy. The paper is organized as follows: in the next section, we address the formalism of computing shear and bulk viscosities in terms of the quark thermal width, which is deduced from the quark self-energy diagram in the framework of real-time thermal field theory (RTF). Next, in results section, the analytic structure of the quark self-energy is rigorously discussed and its contribution to shear and bulk viscosity coefficients of quark matter is also discussed. A summary and conclusion is presented in the last section.

## II. FORMALISM

In the Kubo formalism [65, 66], the shear and bulk viscosities are defined in the Lehmann spectral representation of the two-point correlation functions of operators involving the components of the energy-momentum tensor  $T_{\mu\nu}$  [67]:

$$\begin{pmatrix} \eta \\ \zeta \end{pmatrix} = \lim_{q_0, |\mathbf{q}| \rightarrow 0^+} \frac{1}{q^0} \begin{pmatrix} \frac{1}{20} A_\eta(q^0, \mathbf{q}) \\ \frac{1}{2} A_\zeta(q^0, \mathbf{q}) \end{pmatrix} \quad (1)$$

with the spectral functions  $A_\eta(q)$  and  $A_\zeta(q)$  given by

$$A_\eta(q) = \int d^4x e^{iq \cdot x} \langle [\pi^{ij}(x), \pi^{ij}(0)] \rangle_\beta, \quad (2)$$

$$A_\zeta(q) = \int d^4x e^{iq \cdot x} \langle [\mathcal{P}(x), \mathcal{P}(0)] \rangle_\beta, \quad (3)$$

where

$$\pi^{ij}(x) = T^{ij}(x) - \frac{1}{3} \delta^{ij} T^k_k, \quad (4)$$

$$\mathcal{P}(x) = -\frac{1}{3} T^i_i(x) - c_s^2 T^{00}(x). \quad (5)$$

In the above equations,  $c_s^2$  is the sound velocity and  $\langle (\dots) \rangle_\beta$  denotes an appropriate thermal average. We note here that the second term in the expression for  $\mathcal{P}(x)$  is necessary to account for energy conservation in a quasi-particle

description of the medium, an approximation we use in the present paper — a clear discussion on this issue can be found in Ref. [10].

We use the NJL model to obtain the above correlation functions. The Lagrangian density of the model for  $u$  and  $d$  flavors is of the form

$$\mathcal{L} = \bar{\psi}(i\partial - m_Q)\psi + G [(\bar{\psi}\psi)^2 + (\bar{\psi}i\gamma^5\boldsymbol{\tau}\psi)^2], \quad (6)$$

where  $m_Q = (m_u, m_d)$  is the current quark mass matrix and  $\boldsymbol{\tau} = (\tau^1, \tau^2, \tau^3)$  are the flavor Pauli matrices. The energy-momentum tensor is given in terms of the Lagrangian density by

$$T^{\mu\nu} = -g^{\mu\nu}\mathcal{L} + \frac{\partial\mathcal{L}}{\partial(\partial_\mu\psi)}\partial^\nu\psi = g^{\mu\nu}\mathcal{L} + i\bar{\psi}\gamma^\mu\partial^\nu\psi. \quad (7)$$

The model will be treated in the quasi-particle approximation or, equivalently, in the leading-order approximation in the  $1/N_c$  expansion, where  $N_c = 3$  is the number of colors, which is also equivalent to the traditional Hartree approximation of many-body theory. In this approximation, the thermal spectral functions can be expressed in terms of the quark propagator.

We use the formalism of real-time thermal field theory (RTF) to obtain the correlation functions. In RFT, the two point function of any field-theoretic operator has a  $2 \times 2$  matrix structure reflecting the time ordering with respect to a contour in the complex plane [68]. The relevant matrix can be diagonalized in terms of a single analytic function, which determines completely the dynamics of the corresponding two-point function. In particular, the retarded correlation functions needed for the evaluation of  $A_\eta(q)$  and  $A_\zeta(q)$  can be written in terms of the 11 component of the corresponding two-point functions — see Ref. [69] for details. For example, ignoring for the moment quark-meson fluctuations,  $A_\eta(q)$  can be written as

$$A_\eta(q) = 2 \tanh\left(\frac{\beta q_0}{2}\right) \text{Im} \Pi_{11}(q), \quad (8)$$

with

$$\Pi_{11}(q) = iN_c N_f \int \frac{d^4k}{(2\pi)^4} N(q, k) D_{11}(k) D_{11}(q+k), \quad (9)$$

where  $D_{11}(q)$  is the scalar part of the 11 component quark-propagator matrix (in the zero width case):

$$D_{11}(k) = \frac{-1}{k_0^2 - (\omega_Q^k)^2 + i\epsilon} - 2\pi i \omega_Q^k n_Q(\mathbf{k}) \delta(k_0^2 - (\omega_Q^k)^2). \quad (10)$$

The  $n_Q(\mathbf{k})$  in Eq. (10) is the Fermi-Dirac distribution

$$n_Q(\mathbf{k}) = \frac{1}{1 + e^{\beta\omega_Q^k}}, \quad (11)$$

with  $\omega_Q^k = (\mathbf{k}^2 + M_Q^2)^{1/2}$ , and

$$N(q, k) = \frac{32}{3} k_0 (k_0 + q_0) \mathbf{k} \cdot (\mathbf{k} + \mathbf{q}) - 4 \left[ \mathbf{k} \cdot (\mathbf{k} + \mathbf{q}) + \frac{1}{3} \mathbf{k}^2 (\mathbf{k} + \mathbf{q})^2 \right]. \quad (12)$$

Fig. 1(a) shows this quark-quark loop diagram, which can be considered as a schematic representation of shear viscosity coefficient at the zero frequency and momentum limit. The quark mass  $M_Q$  is the solution of the gap equation

$$M_Q = m_Q + 4N_c N_f G M_Q \int \frac{d^3 \mathbf{k}}{(2\pi)^3} \frac{1 - 2n_Q(\mathbf{k})}{\omega_Q^k}. \quad (13)$$

The temperature-independent part of the integral above is ultraviolet divergent, while the temperature-dependent part, which contains the Fermi-Dirac distribution function  $n_Q(\mathbf{k})$ , is finite. We use a ultraviolet cutoff  $\Lambda$  to regularize the divergent integral, with  $\Lambda$  fitted (together with the other parameters of the model,  $m_Q$  and  $G$ ) to obtain reasonable values for the quark condensate, pion leptonic decay constant and the pion mass in vacuum. The finite integral is integrated without a cutoff.

To proceed with the evaluation of the viscosities, we include the dissipative processes due to quark-meson fluctuations. The fluctuations introduce an imaginary part in the quark self energy giving a thermal width  $\Gamma_Q$  to the quarks; as it stands, with no finite imaginary part in the quark propagator, Eq. (9) leads to divergent viscosities. Adding an on-shell, momentum-dependent thermal width  $\Gamma_Q(k)$  in the quark propagator, one obtains [69] for the shear viscosity the expression

$$\eta = \frac{4N_c N_f}{15T} \int \frac{d^3 \mathbf{k}}{(2\pi)^3} \frac{\mathbf{k}^4 n_Q(\mathbf{k}) [1 - n_Q(\mathbf{k})]}{(\omega_Q^k)^2 \Gamma_Q(\mathbf{k})}. \quad (14)$$

This expression for  $\eta$  is identical to the one obtained from the standard relaxation time approximation [28, 43]. For bulk viscosity, from Eq. (3) we obtain:

$$\zeta = \frac{4N_c N_f}{T} \int \frac{d^3 \mathbf{k}}{(2\pi)^3} \frac{n_Q(\mathbf{k}) [1 - n_Q(\mathbf{k})]}{(\omega_Q^k)^2 \Gamma_Q(\mathbf{k})} \times \left[ \left( \frac{1}{3} - c_s^2 \right) \mathbf{k}^2 - c_s^2 \frac{d}{d\beta^2} (\beta^2 M_Q^2) \right]^2, \quad (15)$$

which is also identical to the one obtained in Ref. [28] which uses the relaxation time approximation.

We evaluate the quark thermal width  $\Gamma_Q(\mathbf{k})$  from the quark-meson ( $QM$ ) loop contributions to the quark self-energy, pictorially represented in Fig 1(b). We need the meson masses and quark-meson couplings. We assume the couplings of the mesons to the quarks are of Yukawa type [70]:

$$\mathcal{L}_{QQ\pi} = ig_{QQ\pi} \bar{\psi} \gamma^5 \boldsymbol{\tau} \cdot \boldsymbol{\pi} \psi, \quad (16)$$

for the  $\pi$  coupling, and

$$\mathcal{L}_{QQ\sigma} = g_{QQ\sigma} \bar{\psi} \sigma \psi, \quad (17)$$

for the  $\sigma$  coupling. Note that the couplings  $g_{QQ\sigma}$  and  $g_{QQ\pi}$  are not bare couplings; they incorporate the effects of dynamical chiral symmetry breaking and as such are different from each other. At high temperatures, when chiral symmetry is restored, they become equal to each other, as we discuss in the next section. The meson masses  $m_M$  and quark-meson couplings  $g_{QQM}$  are calculated from well-known expressions of the NJL model [63]:

$$1 - 2G\Pi_M(\omega^2 = m_M^2) = 0, \quad (18)$$

$$g_{QQM}^2 = \left[ \frac{\partial \Pi_M(\omega^2)}{\partial \omega^2} \right]_{\omega^2 = m_M^2}^{-1}, \quad (19)$$

$$\Pi_M(\omega^2) = 2N_c N_f \int \frac{d^3 \mathbf{k}}{(2\pi)^3} \frac{1 - 2n_Q(\mathbf{k})}{\omega_Q^k} F_M(\omega^2), \quad (20)$$

with

$$F_\pi(\omega^2) = \frac{(\omega_Q^k)^2}{(\omega_Q^k)^2 - \omega^2/4}, \quad (21)$$

$$F_\sigma(\omega^2) = \frac{(\omega_Q^k)^2 - M_Q^2}{(\omega_Q^k)^2 - \omega^2/4}, \quad (22)$$

where  $M_Q$  is the solution of the gap equation in Eq. (13). The integrals in Eq. (20) are to be understood as principal-value integrals when  $\omega^2 > 4M_Q^2$ . Like with the gap equation, the temperature independent part of the integral for  $\Pi_M(\omega^2)$  is divergent, and we use the same cutoff  $\Lambda$  as in the gap equation.

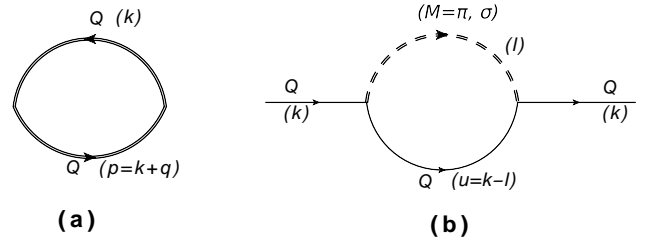


FIG. 1: The diagram (a) represents a schematic one-loop diagram of the quark correlator, which can be obtained from the two-point function of the viscous-stress tensor for the quark constituents. The double-dashed lines for the quark propagators indicate that they have some finite thermal width which can be derived from the quark self-energy diagrams (b) for quark-meson loops (for  $\pi, \sigma$  meson).

Given the meson masses and quark-meson couplings, the quark thermal width is obtained from the imaginary part of the loop diagrams shown in Fig. 1 (b). The off-shell quark self-energy contains four branch cuts on the energy axis, but on-shell only the Landau cut contributes [69] and the result can be written as

$$\Gamma_Q = \sum_{M=\pi, \sigma} \Gamma_{Q(QM)}$$

$$= \left[ \int \frac{d^3\mathbf{l}}{(2\pi)^3} \delta(k^0 + \omega_Q^l - \omega_M^u) \frac{n_Q(\mathbf{l}) + n_M(\mathbf{u})}{4\omega_Q^l \omega_M^u} \right. \\ \left. \times L_{Q(QM)}(k^0, \mathbf{k}; l^0 = -\omega_Q^l, \mathbf{l}) \right]_{k^0 = \omega_Q^k}, \quad (23)$$

where  $\mathbf{u} = \mathbf{k} - \mathbf{l}$ ,  $n_M(\mathbf{k})$  is the Bose-Einstein distribution

$$n_M(\mathbf{k}) = \frac{1}{e^{\beta\omega_M^k} - 1}, \quad (24)$$

with  $\omega_M^k = (\mathbf{k}^2 + m_M^2)^{1/2}$ , and

$$L_{Q(Q\pi)}(k, l) = 3 \frac{4g_{QQ\pi}^2}{M_Q} (M_Q^2 - k \cdot l), \quad (25)$$

$$L_{Q(Q\sigma)}(k, l) = \frac{4g_{QQ\sigma}^2}{M_Q} (M_Q^2 + k \cdot l). \quad (26)$$

Note that use of an on-shell quark thermal width is consistent with the quasi-particle approximation we are using to describe the system.

The last input needed is the sound velocity  $c_s$ , which is required for the evaluation of the bulk viscosity in Eq. (15). It can be obtained from the pressure  $P$  and energy density  $\epsilon$  as:

$$c_s^2 = \left( \frac{\partial P}{\partial \epsilon} \right)_s = \frac{s}{c_V}, \quad (27)$$

where  $s$  is the entropy density and  $c_V$  the specific heat at constant volume:

$$s = \frac{\epsilon + P}{T}, \quad c_V = T \left( \frac{\partial s}{\partial T} \right)_V. \quad (28)$$

The pressure  $P$  and energy density  $\epsilon$  are given in the quasi-particle approximation to the NJL model as

$$\left( \begin{array}{c} P \\ \epsilon \end{array} \right) = 4N_c N_f \int \frac{d^3\mathbf{k}}{(2\pi)^3} n_Q(\mathbf{k}) \left( \begin{array}{c} \mathbf{k}^2/3\omega_Q^k \\ \omega_Q^k \end{array} \right). \quad (29)$$

We note that the use of the quasi-particle approximation for the thermodynamic quantities is consistent with the large  $N_c$  counting [64]. Inclusion of meson loops contributions requires care with respect to thermodynamic consistency.

### III. NUMERICAL RESULTS AND DISCUSSION

The free parameters in the NJL model are the current quark mass  $m_Q$ , the coupling  $G$  and the cutoff mass  $\Lambda$  that is required to regularize vacuum loop diagrams. They are fixed to obtain reasonable vacuum values for the quark condensate  $\langle \bar{u}u \rangle$ , pion leptonic decay constant  $f_\pi$  and the pion mass  $m_\pi$ . With  $m_Q = m_u = m_d = 5$  MeV,  $G\Lambda^2 = 2.14$  and  $\Lambda = 653$  MeV, one obtains:  $\langle \bar{u}u \rangle = (-252 \text{ MeV})^3$ ,  $f_\pi = 94$  MeV and

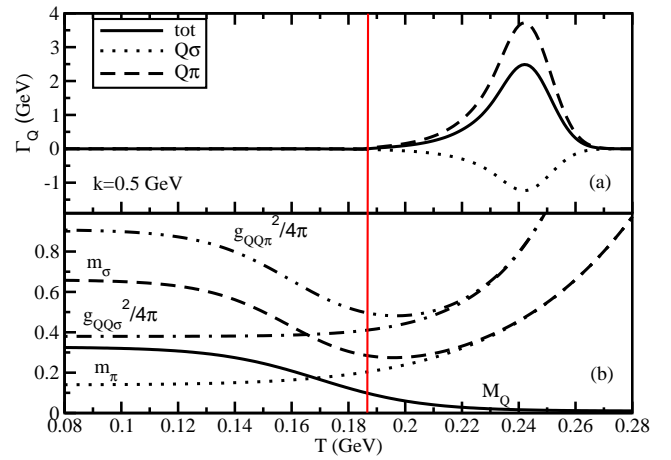


FIG. 2: (Color on-line) (a) Temperature dependence of  $\Gamma_Q$  (solid line) for  $k = 0.5$  GeV and the individual contribution from  $\pi^-$  (dashed line) and  $\sigma^-$  quark loops (dotted line). (b) Temperature dependence of quark mass (solid line), the pion (dotted line), and the sigma (dashed line) meson masses and quark-meson couplings ( $g_{QQ\pi}^2/4\pi$ : dash-dotted line and  $g_{QQ\sigma}^2/4\pi$ : dash-double-dotted line). The straight vertical red line denotes the Mott temperature ( $T_M = 0.187$  GeV).

$m_\pi = 142$  MeV. The vacuum value of the constituent quark mass is  $M_Q = M_u = M_d = 328$  MeV mass and of the  $\sigma$  mass is  $m_\sigma = 663$  MeV.

We start our numerical discussion from on-shell quark thermal width  $\Gamma_Q(\mathbf{k}, T)$ , which we present in the top panel of Fig. (2) for a specific value of the momentum,  $\mathbf{k} = 0.5$  GeV. Also shown are the individual contributions from the  $\pi^-$  and  $\sigma^-$  quark loops. In the lower panel of the figure, we show the temperature dependences of the quark-meson couplings and quark,  $\pi$  and  $\sigma$  masses. The straight vertical red line in the figure denotes the Mott temperature  $T_M$ , at which  $m_\pi(T_M) = 2M_Q(T_M)$ . For the parameter values used in the present paper,  $T_M = 0.187$  GeV. Here one should notice that the numerical strengths of the pion and sigma modes are opposite in sign [36, 70], but the magnitude of the pion mode is approximately three times larger than the magnitude of the sigma mode in the temperature range  $T > T_M$ . In the lower panel of the figure, one should notice that at sufficiently high temperatures, the  $g_{QQ\pi} \simeq g_{QQ\sigma}$  as well as  $m_\sigma \simeq m_\pi$ , a feature due to the chiral symmetry restoration at high temperatures.

It is instructive to examine the invariant-mass  $M$  dependence of the individual contributions  $\Gamma_{Q(Q\pi)}$  and  $\Gamma_{Q(Q\sigma)}$  to  $\Gamma_Q$ ;  $M$  is given by  $M^2 = (k^0)^2 - \mathbf{k}^2$ . Results for  $\mathbf{k} = 0.5$  GeV and three different temperatures are shown in Fig. 3. The Landau-cut regions for quark-pion ( $Q\pi$ ) and quark-sigma ( $Q\sigma$ ) loops of the quark self-energy are respectively  $0 < M < |m_\pi - M_Q|$  and  $0 < M < |m_\sigma - M_Q|$ ; they are identified by the nonzero values of the corresponding  $\Gamma_{QQM}(M)$ 's, as indicated in the figure. Clearly, the Landau-cut is very sensitive to the temperature as it is determined by

the temperature-dependent quark mass  $M_Q$  and meson masses  $m_\pi$  and  $m_\sigma$ . The strengths of the  $\Gamma_{QQM}$  are essentially controlled by the quark-meson coupling constants; please note the different scales in the vertical axes of the different panels. Also, while the threshold condition ( $m_\sigma - 2M_Q \geq 0$ ) for the  $Q\sigma$  loop is satisfied for all temperatures, the corresponding threshold condition for the  $Q\pi$  loop ( $m_\pi - 2M_Q \geq 0$ ) is only satisfied beyond the Mott temperature  $T_M = 0.187$  GeV. This last feature explains the fact that the quark-mass pole, indicated by the vertical dashed lines in the figure, lies outside of the Landau cut for  $Q\pi$  loop at  $T = 0.180$  GeV.

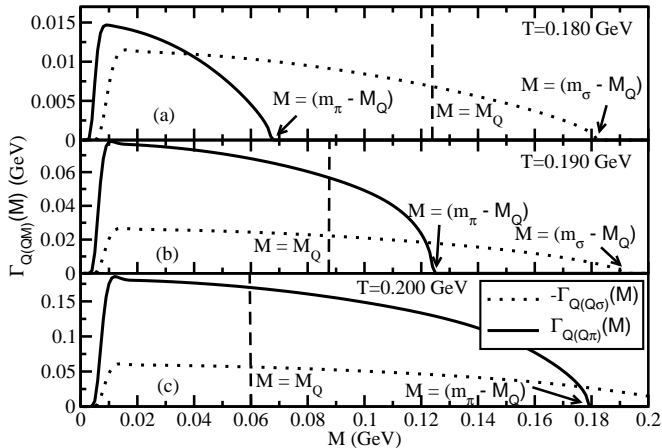


FIG. 3: Invariant mass distribution of the quark thermal width from the  $Q\pi$  (solid line) and  $Q\sigma$  (dotted line) loops for  $|\mathbf{k}| = 500$  MeV for temperatures (a)  $T = 0.180$  GeV, (b)  $0.190$  GeV, and (c)  $0.200$  GeV. The curve for  $\Gamma_{Q(Q\sigma)}(M)$  as been multiplied by  $-1$ .

Next we examine the temperature dependence of  $\Gamma_Q$  and of its inverse, the collisional time  $\tau_Q = 1/\Gamma_Q$ , for three different values of momentum; the results are shown in Fig. 4. The peak position and strength of the temperature dependence of  $\Gamma_Q$  is strongly momentum dependent, a feature that reflects the absorption and emission processes of the quark interacting with mesonic modes; recall that  $\Gamma_{QQM}$  physically means the on-shell probability of forward and inverse scattering between a quark  $Q$  and the mesonic modes  $M$  [71]. In forward scattering,  $Q$  may be transformed to a thermalized  $M$  by absorbing a thermalized anti-quark  $\bar{Q}$ , while in the inverse process, an off-equilibrated  $Q$  may be regenerated via  $M \rightarrow Q\bar{Q}$  dissociation. We should note as well that  $\Gamma_Q$  decreases and ultimately goes to zero for large temperatures; the temperature, for which it tends to be numerically zero, depends of course on  $\mathbf{k}$  and is determined by the temperature-dependent quark and meson masses and couplings. The implication of  $\Gamma_Q$  decreasing with  $T$  for large  $T$  has the implication that  $\eta$  and  $\zeta$  will increase with  $T$ , and again, the value of  $T$  where it starts to increase and the rate of increase depend on the parameters of the model.

When considering the collisional time, shown in the

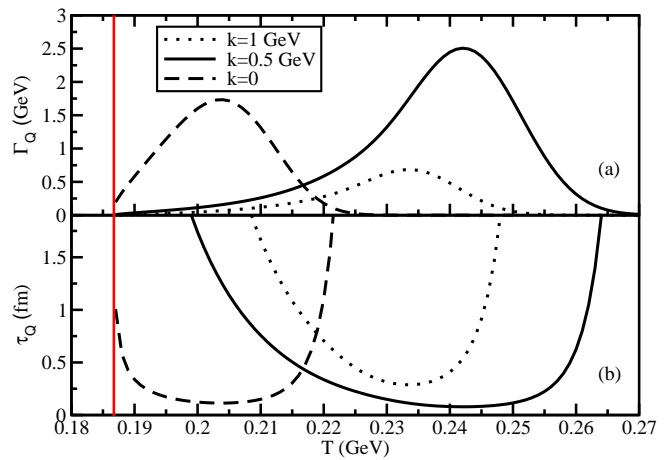


FIG. 4: (Color on-line) (a) Temperature dependence of the quark thermal width  $\Gamma_Q$  and (b) collisional time  $\tau_Q = 1/\Gamma_Q$  for three different values of momentum:  $\mathbf{k} = 0$  (dashed line),  $0.5$  GeV (solid line), and  $1$  GeV (dotted line). The vertical red line indicates the Mott temperature.

lower panel of Fig. 4, one can compare time scales of dissipation with the typical evolution time  $\Delta\tau$  of the matter produced in a HIC, which is  $\Delta\tau \simeq 1 - 10$  fm. One can clearly identify well-defined temperature ranges for which  $\tau_Q < \Delta\tau$ , i.e. for which the propagating quark in the medium suffers sufficient dissipation by scattering with the thermalized constituents of the medium.

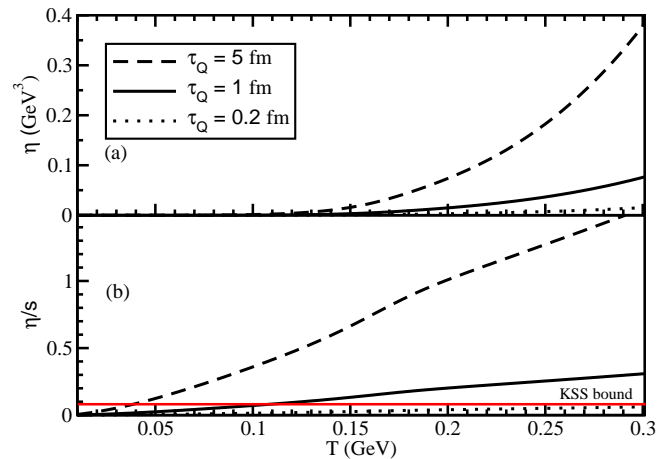


FIG. 5: (Color on-line) (a) Temperature dependence of  $\eta$  and (b)  $\eta/s$  for different values of constant collisional time:  $\tau_Q = 5$  fm (dashed line),  $1$  fm (solid line), and  $0.2$  fm (dotted line). The straight horizontal red line indicates the KSS bound,  $\eta/s = 1/4\pi$ .

Before using the full temperature- and momentum-dependent  $\Gamma_Q(k)$  in Eqs. (14) and (15), we have calculated the temperature dependence of  $\eta$  and  $\zeta$  for a constant value of  $\tau_Q = 1/\Gamma_Q$ . Although the temperature and momentum dependence of  $\Gamma_Q$  will modify somewhat the results for the viscosities, the calculation with

a constant  $\Gamma_Q$  will bring insight regarding the integrands in Eqs. (14) and (15) when  $\Gamma_Q$  can be taken out of the integrals. In Fig. 5 we show the corresponding results for  $\eta$  and  $\eta/s$ , for different values of  $\tau_Q$ . While  $\eta$  is a monotonically increasing function of  $T$ , the ratio  $\eta/s$  exhibits two different rates of increase in two different temperature domains, which are associated with two different phases.

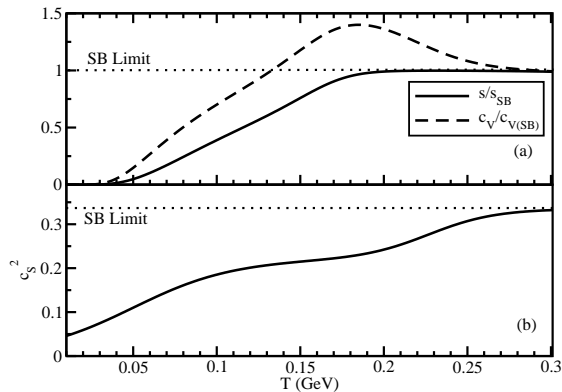


FIG. 6: (a) The temperature dependence of entropy density, normalized by Stephan-Boltzmann (SB) limiting value  $s_{SB}$ , given in Eq. (30). (b) The squared speed of sound  $c_s^2$  as a function of the temperature. Straight horizontal dotted lines stand for the corresponding SB limits.

The observed change in the rate of increase of  $\eta/s$  with the temperature can be understood from the temperature dependence of  $s$ , normalized by the Stephan-Boltzmann (SB) limiting value:

$$s_{SB} = 4N_c N_f \left(\frac{7}{2}\right) \left(\frac{\pi^2}{90}\right) T^3. \quad (30)$$

One observes in Fig. 6(a) that the rate of increment in  $s/s_{SB}$  mainly changes around  $T \approx 0.175 - 185$  GeV; above this temperature, the entropy density of quark matter becomes almost identical with the SB limiting value, which is denoted by straight horizontal dotted line in the figure. It is important to note that we are taking into account the contributions of the quarks only in the expression for  $s_{SB}$ ; including gluon degrees of freedom will increase  $s_{SB}$  by a factor roughly equal to 1.75 (for  $N_f = 2$ ). Being proportional to the slope of  $s$ , the specific heat  $c_V$  is magnifying the transition by exhibiting a smooth hump structure around  $T \approx 0.175 - 185$  GeV as shown in Fig. 6(a). Such a behavior of  $c_V$  has been obtained also in other recent calculations employing the NJL model, as e.g. in Refs. [34, 72, 73]. Note, however, that the maximum of  $c_V$  is still well below the corresponding SB limit in QCD which, of course, includes gluon degrees of freedom and is thereby 1.75 larger than the pure-quark SB limit. This is a welcome feature as lattice QCD simulations [48] show no indication that the specific heat exceeds the QCD SB limit at any temperature. For calculating the bulk viscosity, we have obtained

$c_s^2$  using Eq. (27); its temperature dependence is shown in Fig. 6(b). Assuming the system is not very far from equilibrium, all thermodynamical quantities are obtained for non-interacting system of quark matter, although a finite (not zero) probability of quark-meson interaction has to be considered for getting a non-divergent values of transport coefficients.

Fig. 7 shows results for the temperature dependence of  $\zeta$  and  $\zeta/s$ , for different constant values of  $\tau_Q$ . A non-monotonic temperature dependence of  $\zeta$  is obtained, with a distinctive two-peak structure at temperatures  $T \approx 0.150 - 0.160$  GeV and  $T \approx 0.210 - 0.220$  GeV. Similar double-peak structure for  $\zeta$  was obtained in Ref. [58]. Note that the first peak is located at a temperature below the Mott temperature and will not be seen (Fig. 10) when using the full temperature and momentum dependence of  $\Gamma_Q(\mathbf{k}, T)$ .

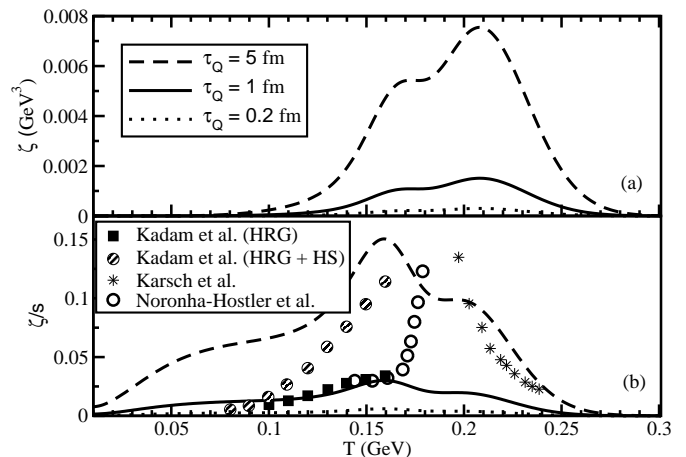


FIG. 7: (a) Temperature dependence of  $\zeta$  and (b)  $\zeta/s$  for different values of constant  $\tau_Q$ . In the lower panel, also shown are results from the literature: Ref. [41] (filled circles and squares), Ref. [54] (open circles), Ref. [53] (stars).

The double-peaked structure is clearly the result of a competition between the two conformality breaking terms in the integrand of Eq. (15),  $1/3 - c_s^2$  and  $d(\beta^2 M_Q^2)/d\beta^2$ : the first is associated with  $c_s^2 \neq 1/3$  and the second is associated with the bulk mass transport [28]. To get a graphical understanding of the competition, let us define auxiliary quantities containing these terms:  $A = 1/3 - c_s^2$ ,  $B = d(\beta^2 M_Q^2)/d\beta^2$ ,  $C = A \mathbf{k}^2$ ,  $D = c_s^2 B$  and  $E = (C - D)^2$ . These quantities are plotted in the different panels in Fig. 8.

The key feature here is that the  $C$  (with any fixed momentum) and  $D$  curves intersect each other at three different points; therefore,  $E = (C - D)^2$  possesses three nodes (minima) and, of course, two maxima along the  $T$ -axis. These two maxima remain when  $E = E(\mathbf{k})$  is integrated over  $\mathbf{k}$  in Eq. (15) and the two-peak structure is clearly understood in these terms. Of course, if  $M_Q$  is temperature independent, then one has only one peak, as the lower peaks in Figs. 7 and 8(c) will not appear.

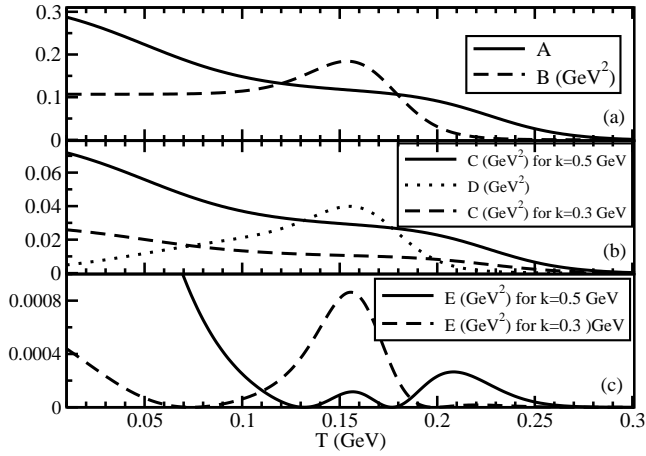


FIG. 8: Temperature dependence of the auxiliary quantities defined in the text. Panel (a):  $A = 1/3 - c_s^2$  (solid line) and  $B = d(\beta^2 M_Q^2)/d\beta^2$  (dashed line). Panel (b):  $C = A \mathbf{k}^2$ , for  $|\mathbf{k}| = 0.5$  GeV (solid line) and  $|\mathbf{k}| = 0.3$  GeV (dashed line),  $D = c_s^2 B$  (dotted line). Panel (c):  $E = (C - D)^2$  for  $|\mathbf{k}| = 0.5$  GeV (solid line) and  $|\mathbf{k}| = 0.3$  GeV (dashed line).

Likewise, as seen in the lower panel of Fig. 7, the ratio  $\zeta/s$  also presents a non-monotonic behavior. For the sake of comparison, Fig. 7(b) also displays results from the literature.

Finally, we present results for the viscosities and viscosity to entropy density ratios with the full momentum dependence of the quark thermal width  $\Gamma_Q(\mathbf{k})$ . It is important to reiterate that our results have physical significance only within a limited range of temperatures, approximately  $T_M < T < 0.240$  GeV. The lower limit is due to the fact that in the NJL model, when using the on-shell thermal width, finite viscosities are obtained for temperatures  $T$  larger than the Mott temperature  $T_M$  because  $\Gamma_Q(k)$  is nonzero only for  $T > T_M$  in this case. As discussed earlier, the off-shell quark self-energy contains four branch cuts on the energy axis, but on-shell only the Landau cut contributes. The upper limit is not a precise limit, but it is related to the lack of asymptotic freedom in the NJL model; it is known that the large temperature behavior of viscosities in QCD, particularly of bulk viscosity, is very different from the one derived from a non-gauge, contact-interaction model [10]. Given this proviso, we discuss next our results for the temperature dependence of  $\eta$  and  $\eta/s$ , and  $\zeta$  and  $\zeta/s$ ; they are presented respectively in Figs. 9 and 10.

First of all, one notices in Figs. 9 and 10 that the use of the full temperature dependence of  $\Gamma_Q(k)$  restricts the domain of temperatures where finite viscosities are obtained. Our numerical values of  $\eta$  and  $\eta/s$  within the temperature range  $T_M < T < 0.240$  GeV, are quite close to some earlier estimates in Refs. [26, 28, 32, 34, 36, 45]. Similarly, Fig. (10) shows fair agreement of our calculation of  $\zeta/s$  with some earlier results of Refs. [28, 34, 53, 58].

The interesting two-peak structure in  $\zeta$  shown in

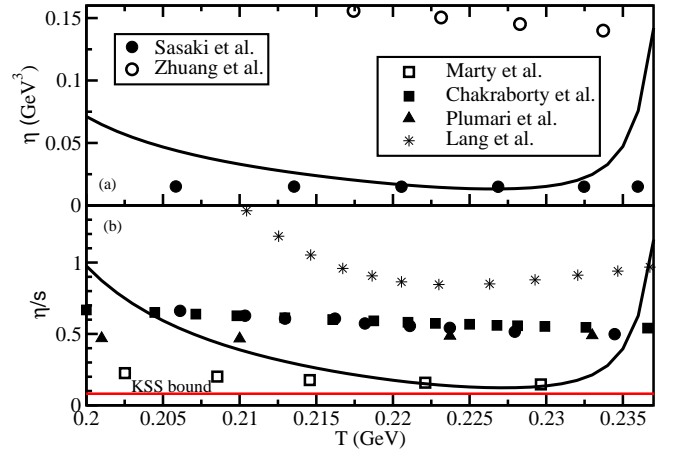


FIG. 9: (Color on-line) (a) Temperature dependence of  $\eta$  and (b)  $\eta/s$  using the full momentum dependence of the quark thermal width  $\Gamma_Q(\mathbf{k})$ . Comparison with results from the literature: Ref. [26] (filled circles), Ref. [45] (open circles), Ref. [34] (open squares), Ref. [28] (filled squares), Ref. [32] (triangles), Ref. [36] (stars).

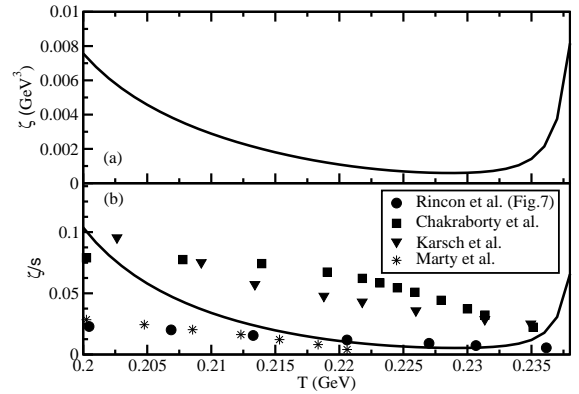


FIG. 10: (a) Temperature dependence of  $\zeta$  and (b)  $\zeta/s$  using the full momentum dependence of the quark thermal width  $\Gamma_Q(\mathbf{k})$ . Comparison with results from the literature: Ref. [58] (circles), Ref. [28] (squares), Ref. [53] (triangles), Ref. [34] (stars).

Fig. (7) is not visible here because, as discussed above, the first peak is below the Mott temperature. In addition, the figures show that the viscosities have a rapid increase with temperature for  $T \geq 0.235$  GeV. This is due to the fact that for high temperatures, the contributions from quark-meson fluctuations to  $\Gamma_Q(k)$  decrease rapidly for large  $T$ , as shown in the top panel of Fig. 2. At higher temperatures, quark-quark and quark-gluon scatterings will become more important than quark-meson scattering. To include such processes, one would probably need a model that incorporates asymptotic freedom, as already mentioned in the previous paragraph. As our focus of interest in the present is on the contributions from quark-meson thermal fluctuations, we reserve for a future publication the investigation of the contributions

of quark-quark and quark-gluon processes to viscosities.

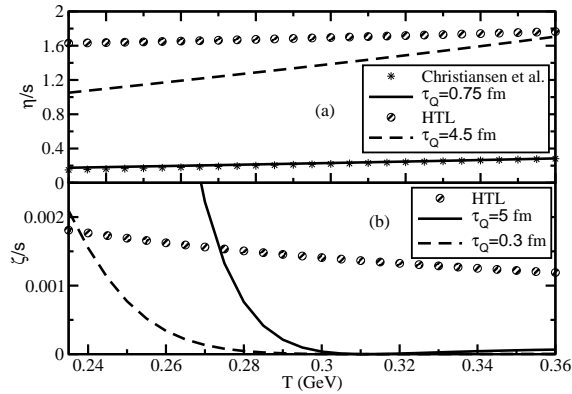


FIG. 11:  $\eta/s$  (a) and  $\zeta/s$  (b) at high temperature domain. HTL (circles) and FRG (stars) estimations of  $\eta/s$  by Arnold et al. [9] and Christiansen et al. [37] are compared with  $\eta/s$  of Eq. (14) at  $\tau_Q = 4.5$  fm (dashed line) and  $\tau_Q = 0.75$  fm (solid line). While HTL (circles) estimation of  $\eta/s$  by Arnold et al. [10] is compared with  $\zeta/s$  of Eq. (15) at  $\tau_Q = 0.3$  fm (dashed line) and  $\tau_Q = 5$  fm (solid line).

We conclude with a discussion of the high-temperature behavior of  $\eta/s$  and  $\zeta/s$  by contrasting results from the literature and what one would obtain from our Eqs. (14) and (15) when using finite values for the collisional time  $\tau_Q$ . Fig. (11) is showing results for these ratios for  $T > 0.240$  GeV from hard thermal loop (HTL) calculations [9, 15, 21] and from a functional renormalization group (FRG) calculation for pure Yang-Mills theory [37]. For  $\eta/s$  we note that the HTL and FRG results are markedly different. The FRG result is almost identical to the one obtained from Eq. (14) with  $\tau_Q = 0.75$  fm as seem to match very well with our result shown in Fig. (9)(b) from temperatures around  $T = 0.23$  GeV. On the other hand, for  $\zeta/s$  there are qualitative and quantitative difference between the HTL results from those from Eq. (15) for the two values of  $\tau_Q$  used—there are no FRG results available for  $\zeta/s$ . The discrepancies are significant and clearly further studies are required.

#### IV. SUMMARY AND PERSPECTIVES

In summary, we have investigated the temperature dependence of the quark-matter shear  $\eta$  and bulk  $\zeta$  viscosities and their ratios to the entropy density  $s$ . The focus of interest was on the contributions from  $Q\pi$  and  $Q\sigma$  fluctuations to the on-shell quark thermal width  $\Gamma_Q$ , a crucial ingredient in the calculation of viscosities. We calculated  $\Gamma_Q(\mathbf{k}, T)$  from the imaginary part of the quark self-energy arising from  $Q\pi$  and  $Q\sigma$  loops using temperature-dependent quark and meson masses and quark-meson couplings. We have investigated in detail the Landau-cut structure of the quark self-energy using real-time thermal

field-theory. The temperature dependence of masses and coupling constants were obtained in the NJL model in the quasi-particle approximation. The entropy density and the speed of sound, which is needed to calculate  $\zeta$ , were also obtained in the NJL model within the quasi-particle approximation.

The temperature dependence of the masses and quark-meson couplings non-trivially influences the Landau-cut structure of the quark self-energy. The quark thermal width, calculated from the on-shell quark self-energy, becomes non-zero and non-negligible within a range of temperature and momentum where the quark pole is situated well inside the Landau-cut. When using a temperature- and momentum-independent quark thermal width  $\Gamma_Q$ , a monotonically increasing shear viscosity as a function of temperature was obtained, whereas, the bulk viscosity exhibits a two-peak structure near the phase transition temperature, reflecting the competition between conformality breaking terms related with the speed of sound in the medium and the bulk mass transport. On the other hand, when the full temperature- and momentum-dependent thermal width is used, finite viscosities are obtained only for temperatures larger than the Mott temperature  $T_M = 0.187$  GeV. In addition, for high temperatures, due to rapidly increasing mesonic masses and decreasing of the constituent quark mass, the probability for quark-meson fluctuations become negligible and the viscosities increase considerable and other processes not related to quark-meson processes take place. Between the two extremes, our results for the  $\eta/s$  and  $\zeta/s$  are in fair agreement with results from the literature, although marked differences can be observed.

Future work includes the investigation of viscosities at high temperatures by the introduction of quark-quark and quark-gluon processes. Of course, agreement with standard perturbative QCD results are expected when using interactions that incorporate the property of asymptotic freedom of QCD. At low temperatures, when the medium is dominated by pions and low-mass resonances [38], the NJL model can be used to obtain pure meson-meson interactions, deduced e.g. via the bosonization technique of NJL model, and results are expected to be very close to the standard results for the viscosities of hadronic matter.

**Acknowledgment:** Work partially financed by Fundação de Amparo à Pesquisa do Estado de São Paulo - FAPESP, Grant Nos. 2009/50180-0 (G.K.), 2012/16766-0 (S.G.), and 2013/01907-0 (G.K.); Conselho Nacional de Desenvolvimento Científico e Tecnológico - CNPq, Grant No. 305894/2009-9 (G.K.). T.C.P and F.E.S. are supported by scholarships from Conselho Nacional de Desenvolvimento Científico e Tecnológico - CNPq. V.R. is supported by the Alexander von Humboldt Foundation. We thank Dirk H. Rischke for a careful reading of an earlier version the manuscript and valuable comments.

- 
- [1] P. Romatschke and U. Romatschke, Phys. Rev. Lett. **99**, 172301 (2007).
- [2] M. Luzum and P. Romatschke, Phys. Rev. C **78**, 034915 (2008).
- [3] H. Song and U. W. Heinz, Phys. Lett. B **658**, 279 (2008).
- [4] H. Song and U. W. Heinz, Phys. Rev. C **78**, 024902 (2008).
- [5] V. Roy, A. K. Chaudhuri, and B. Mohanty, Phys. Rev. C **86**, 014902 (2012).
- [6] H. Niemi, G. S. Denicol, P. Huovinen, E. Molnar, and D. H. Rischke, Phys. Rev. C **86**, 014909 (2012).
- [7] U. Heinz, C. Shen, and H. Song, AIP Conf. Proc. **1441**, 766 (2012).
- [8] B. Schenke, S. Jeon, and C. Gale, Phys. Rev. C **85**, 024901 (2012).
- [9] P. B. Arnold, G. D. Moore, and L. G. Yaffe, J. High Energy Phys. 11 (2000) 001; J. High Energy Phys. 05 (2003) 051.
- [10] P. B. Arnold, C. Dogan, and G. D. Moore, Phys. Rev. D **74**, 085021 (2006).
- [11] A. Dobado and S.N. Santalla, Phys. Rev. D **65**, 096011 (2002).
- [12] A. Dobado and F. J. Llanes-Estrada, Phys. Rev. D **69**, 116004 (2004).
- [13] A. Muronga, Phys. Rev. C **69**, 044901 (2004).
- [14] A. Nakamura and S. Sakai, Phys. Rev. Lett. **94**, 072305 (2005).
- [15] L. P. Csernai, J. I. Kapusta, and L. D. McLerran, Phys. Rev. Lett. **97**, 152303 (2006).
- [16] T. Hirano and M. Gyulassy Nucl. Phys. A **769**, 71 (2006).
- [17] H. B. Meyer, Phys. Rev. D **76**, 101701 (2007); Phys. Rev. D **82**, 054504 (2010).
- [18] J. W. Chen, Y. H. Li, Y. F. Liu, and E. Nakano, Phys. Rev. D **76**, 114011 (2007).
- [19] D. Fernandez-Fraile and A. Gomez Nicola, Eur. Phys. J. A **31**, 848 (2007); Eur. Phys. J. C **62**, 37 (2009); Int. J. Mod. Phys. E **16**, 3010 (2007).
- [20] Z. Xu, C. Greiner, and H. Stocker, Phys. Rev. Lett. **101**, 082302 (2008).
- [21] J. I. Kapusta, *Relativistic Nuclear Collisions*, Landolt-Bornstein New Series, Vol. I/23, ed. R. Stock (Springer-Verlag, Berlin Heidelberg 2010).
- [22] Z. Xu and C. Greiner, Phys. Rev. C **79**, 014904 (2009).
- [23] K. Itakura, O. Morimatsu, and H. Otomo, Phys. Rev. D **77**, 014014 (2008).
- [24] G. Ferini, M. Colonna, M. Di Toro, and V. Greco, Phys. Lett. B **670**, 325 (2009).
- [25] V. Greco, M. Colonna, M. Di Toro, and G. Ferini, Prog. Part. Nucl. Phys. **65**, 562 (2009).
- [26] C. Sasaki and K. Redlich, Nucl. Phys. A **832**, 62 (2010).
- [27] J.W. Chen, C.T. Hsieh, and H. H. Lin, Phys. Lett. B **701**, 327 (2011).
- [28] P. Chakraborty and J. I. Kapusta, Phys. Rev. C **83**, 014906 (2011).
- [29] J. Peralta-Ramos and G. Krein, Phys. Rev. C **84**, 044904 (2011); Int. J. Mod. Phys. Conf. Ser. 18 (2012) 204.
- [30] R. Lang, N. Kaiser, and W. Weise, Eur. Phys. J. A **48**, 109 (2012).
- [31] S. Mitra, S. Ghosh, and S. Sarkar Phys. Rev. C **85**, 064917 (2012).
- [32] S. Plumari, A. Puglisi, F. Scardina, and V. Greco, Phys. Rev. C **86**, 054902 (2012).
- [33] S. Sarkar, Adv. High Energy Phys. **2013**, 627137 (2013).
- [34] R. Marty, E. Bratkovskaya, W. Cassing, J. Aichelin, and H. Berrehrh, Phys. Rev. C **88**, 045204 (2013).
- [35] S. Ghosh, A. Lahiri, S. Majumder, R. Ray, S. K. Ghosh, Phys. Rev. C **88**, 068201 (2013).
- [36] R. Lang and W. Weise Eur. Phys. J. A **50**, 63 (2014).
- [37] N. Christiansen, M. Haas, J.M. Pawlowski, N. Strodthoff, Phys. Rev. Lett. **115**, 112002 (2015).
- [38] S. Ghosh, G. Krein, S. Sarkar, Phys. Rev. C **89**, 045201 (2014).
- [39] N. Sadooghi and F. Taghinavaz, Phys. Rev. D **89**, 125005 (2014).
- [40] S. Ghosh, Phys. Rev. C **90** 025202 (2014).
- [41] G. P. Kadam and H. Mishra, Nucl. Phys. A **934**, 133 (2015); arXiv:1506.04613 [hep-ph].
- [42] S. K. Ghosh, S. Raha, R. Ray, K. Saha, and S. Upadhaya, Phys. Rev. D **91**, 054005 (2015).
- [43] S. Gavin, Nucl. Phys. **A435**, 826 (1985).
- [44] M. Prakash, M. Prakash, R. Venugopalan, and G. Welke, Phys. Rep. **227**, 321 (1993).
- [45] P. Zhuang, J. Hufner, S. P. Klevansky, and L. Neise, Phys. Rev. D **51**, 3728 (1995).
- [46] P. Rehberg, S.P. Klevansky, and J. Hufner, Nucl. Phys. **A608**, 356 (1996).
- [47] P. Kovtun, D. T. Son, and O. A. Starinets, Phys. Rev. Lett. **94**, 111601 (2005).
- [48] A. Bazavov *et al.* (HotQCD Collaboration), Phys. Rev. D **90**, 094503 (2014).
- [49] S. Borsanyi, Z. Fodor, S. D. Katz, S. Krieg, C. Ratti, and K Szabó, J. High Energy Phys. 01 (2012) 138.
- [50] H. B. Meyer, Phys. Rev. Lett. **100**, 162001 (2008).
- [51] K. Paech and S. Pratt, Phys. Rev. C **74**, 014901 (2006).
- [52] D. Kharzeev and K. Tuchin, J. High Energy Phys. 09 (2008) 093
- [53] F. Karsch, D. Kharzeev, and K. Tuchin, Phys. Lett. B **663**, 217 (2008).
- [54] J. Noronha-Hostler, J. Noronha and C. Greiner, Phys. Rev. Lett. **103**, 172302 (2009).
- [55] C. Sasaki and K. Redlich, Phys. Rev. C **79**, 055207 (2009).
- [56] A. Dobado, F.J.Llanes-Estrada, J. Torres Rincon, Phys. Lett. B **702**, 43 (2011).
- [57] V. Chandra, Phys. Rev. D **84**, 094025 (2011); Phys. Rev. D **86**, 114008 (2012).
- [58] A. Dobado and J. Torres Rincon, Phys. Rev. D **86**, 074021 (2012).
- [59] S. Mitra and S. Sarkar, Phys. Rev. D **87**, 094026 (2013); S. Mitra, S. Gangopadhyaya, and S. Sarkar, Phys. Rev. D **91**, 094012 (2015).
- [60] X. Shi-Song, Z. Le, G. Pan-Pan, H. De-Fu, Chin. Phys. C **38**, 054101 (2014).
- [61] K. Saha and S. Upadhaya, arXiv:1505.00177 [hep-ph].
- [62] Y. Nambu and G. Jona-Lasinio, Phys. Rev. **122**, 345 (1961); Phys. Rev. **124**, 246 (1962).
- [63] U. Vogl and W. Weise, Prog. Part. Nucl. Phys. **27**, 195 (1991); S. P. Klevansky, Rev. Mod. Phys. **64**, 649 (1992); T. Hatsuda and T. Kunihiro, Phys. Rep. **247**, 221 (1994); M. Buballa, Phys. Rep. **407**, 205 (2005).
- [64] R. Lang, N. Kaiser, and W. Weise, Eur. Phys. J. A **51**,

- 127 (2015).
- [65] D. N. Zubarev, *Non-equilibrium statistical thermodynamics* (New York, Consultants Bureau, 1974).
- [66] R. Kubo, J. Phys. Soc. Jpn. **12**, 570 (1957).
- [67] A. Hosoya, M.-A. Sakagami, and M. Takao, Ann. Phys. (N.Y.) **154**, 229 (1984).
- [68] M. Le Bellac, *Thermal Field Theory* (Cambridge University Press, Cambridge, England, 2000).
- [69] S. Ghosh, Int. J. Mod. Phys. A **29**, 1450054 (2014).
- [70] E. Quack and S. P. Klevansky, Phys. Rev. C **49**, 6 (1994).
- [71] H.A. Weldon, Phys. Rev. D **28**, 2007 (1983).
- [72] S. Chatterjee and K. A. Mohan, Phys. Rev. D **85**, 074018 (2012).
- [73] A. Bhattacharyya, P. Deb, S. K. Ghosh, R. Ray, and S. Sur, Phys. Rev. D **87**, no. 5, 054009 (2013).